# Journal of Materials Chemistry C

Accepted Manuscript


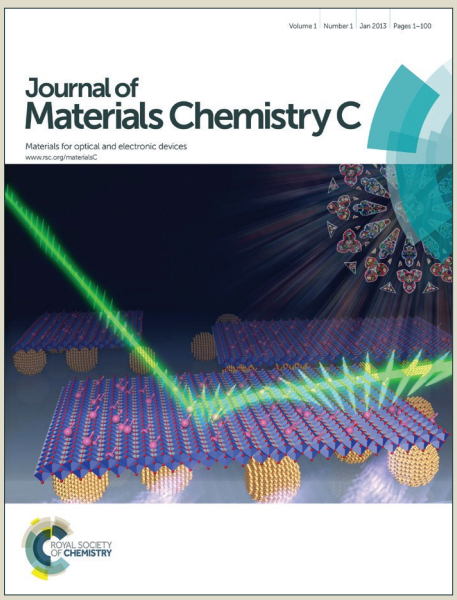





ROYAL SOCIETY OF CHEMISTRY

www.rsc.org/materialsC

Journal Name

RSCPublishing

ARTICLE

# Inverted and Large Flexible Organic Light-Emitting Diodes with Low Operating Voltage

Cite this: DOI: 10.1039/xoxxoooooox

Xun Tang,‡ Lei Ding,‡ Yan-Qiu Sun, Yue-Min Xie, Ya-Li Deng, Zhao-Kui Wang*, and Liang-Sheng Liao *

Received ooth January 2012,
Accepted ooth January 2012

DOI: 10.1039/xoxxoooooox

www.rsc.org/

Green phosphorescent inverted organic light-emitting diodes (IOLEDs) with 1,4,5,8,9,11–hexaazatriphenylene-hexacarbonitrile (HAT-CN)/Aluminium/n-doped 4,7-diphenyl-1,10-phenanthroline (Bphen) used as electron injection layer (EIL) was demonstrated. The IOLED shows the lowest driving voltage of 4.5 V at 10000 cd/m$^2$ to date. The electron injecting effects of different interlayer are further investigated by ultraviolet photoelectron spectroscopy (UPS) and evaluating the electron injection efficiency. For application in large-size OLEDs, a 120×120 mm$^2$ flexible IOLED was successfully fabricated based on this inverted structure.

## Introduction

Flexible organic light-emitting diodes (OLEDs) for display with thin film transistors (TFTs) in each pixel are desired for full color display.[1,2] It is considered that oxide TFTs are more appealing than other various kinds of TFTs for large-size panels because of their low temperature processing, good uniformity, and flexibility under repeated bending along with high carrier mobility.[3] Since the oxide TFTs operated in the *n*-channel mode, inverted OLEDs (IOLEDs) with a bottom cathode are better than conventional OLEDs to integrate with the *n*-channel oxide TFTs. Moreover, in a typical IOLED device, the air-unstable active metal electron injection layer is placed at the bottom of the device, which would improve the device lifetime effectively. Nevertheless, it is well known that there are some difficulties to form bottom cathode having good electron injection characteristics.

To date, IOLEDs still face many problems. The major issue in IOLEDs is the poor performance of the electron injection from the transparent bottom cathode to electron transporting layer (ETL). Transparent metal oxide (ITO or IZO) have high work functions (>4.3 eV), while the lowest unoccupied molecular orbital (LUMO) level of electron transporting materials (ETMs) is in the region of 2.8-3.3 eV,[5] resulting in large energy barriers from ITO cathode to the ETL. Many kinds of methods have been proposed to enhance the electron injection in the inverted structures.[6-14] For example, ETL doped with *n*-type dopant has been successfully applied to obtain good electron injection from ITO to ETL.[15-20] Lee *et al*. developed an organic *p*-*n* junction onto ITO, which showed efficient charge generation under a reverse bias and efficient electron injection.[21] However, most of reports about bottom IOLEDs still show higher driving voltage, which will cause large power loss.

In this paper, we report a novel *p*-*n* junction structure, 1,4,5,8,9,11–hexaazatriphenylene-hexacarbonitrile (HAT-CN)/Al/*n*-doped 4,7-diphenyl-1,10-phenanthroline (Bphen), as an efficient electron injection layer (EIL) in inverted OLEDs. The EIL structure is proved to improve the electron injection efficiently, which can reduce the operating voltage dramatically. As a result, the green phosphorescent IOLEDs with HAT-CN/Al/Bphen: Li EIL demonstrated very low driving voltage of 4.5 V at 10000 cd/m$^2$, which is the lowest value of green phosphorescent IOLEDs to date. Meanwhile, a large-size (120×120 mm$^2$) green phosphorescent IOLED flexible panel is successfully fabricated by using this novel EIL interfacial layer.

## Experimental

### Materials and Devices Fabrication.

IOLEDs were fabricated by thermal evaporating on pre-cleaned glass substrates under a base vacuum of around $10^{-6}$ torr. Current density-voltage (*J*-*V*) and luminance-voltage (*L*-*V*) characteristics are carried out using Keithley 4200 Source Meter and PR-670 photometer in air at room temperature. The ultraviolet photoelectron spectroscopy (UPS) was carried out to evaluate the work function of ITO, ITO/HAT-CN and ITO/HAT-CN/Al films, respectively.

The structure of the IOLED is ITO/EIL/1,3,5- tri(m-pyrid-3-yl-phenyl) benzene (TmPyPB) (40 nm)/4,4'-N,N-

dicarbazolylbiphenyl (CBP): fac–tris (2-phenylpyridine) iridium(III) ($Ir(ppy)_3$) (15 nm, 7%)/1, 3, 5-Triazo-2, 4, 6-triphosphorine-2, 2, 4, 4, 6, 6-tetrachloride (TAPC) (45 nm)/HAT-CN (10 nm)/Al, where CBP: $Ir(ppy)_3$, TAPC, TmPyPB and HAT-CN are used as emitting layer, hole transport layer, electron transport layer and hole injection layer, respectively. Three different EILs of Bphen: Li, HAT-CN/Bphen: Li and HAT-CN/Al/Bphen: Li were selected to investigate their functions on the performance of the IOLEDs. LiH was used as the *n*-dopant in the devices based on the decomposition mechanism of $2LiH \rightarrow 2Li+H_2$. Figure 1 shows the device structure and chemical structure of the materials used for the IOLED.

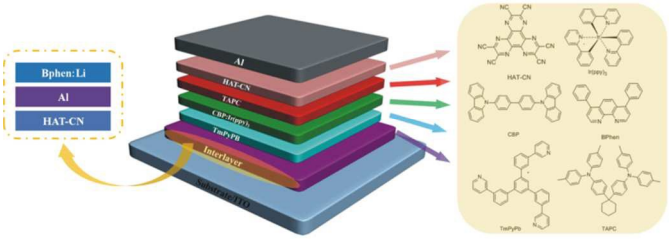


**Fig. 1** Device structure and chemical structures of the materials used in IOLEDs.

**Measurements and Characterization.**

The film thickness and the deposition rate of each material in the IOLEDs were monitored *in situ* using an oscillating quartz thickness monitor. A photometer (Photo Research Spectra Scan PR 655) was used to measure the electroluminescent (EL) spectra and the Commission International de I'Eclairage (CIE) coordinates of all devices. The current density-voltage (*J-V*) characteristic was measured by combined with a constant current source (Keithley 2400 Source Meter). Ultraviolet photoelectron spectroscopy (UPS) was carried out to evaluate the energy levels of the functional materials.

## Results and Discussion

Figure 2 (a) shows the *J-V-L* characteristics of the inverted OLEDs with different EILs. Among three devices, the EIL with a structure of HAT-CN/Al/Bphen: Li based IOLED shows the lowest driving voltage than the devices with EILs of Bphen: Li and HAT-CN/Bphen: Li at the same current density. It indicates that electrons can be injected and transported effectively from the bottom ITO cathode to the light emitting layer in the HAT-CN/Al/BPhen: Li based device. In details, the driving voltage

of device with HAT-CN/Al/Bphen: Li EIL shows extremely low driving voltage: at 100 $cd/m^2$, the voltage is only 3.3 V; at brightness of 1000 $cd/m^2$, the voltage is slightly increased to 3.7 V and even at high brightness of 10000 $cd/m^2$, the voltage was only 4.5 V, which is the lowest driving voltage for reported IOLEDs to date. The corresponding power efficiency-luminance characteristics in three devices are shown in Figure 2(b). The electroluminescence performance of the IOLEDs devices with different EILs are summarized in Table 1. Bphen: Li based device shows the inferior power efficiency due to the inefficient electron injection and transport. With introducing HAT-CN thin layer, the driving voltage slightly rised due to the increased device thickness. By inserting an ultra-thin Al layer, HAT-CN/Al/Bphen: Li based device shows the best power efficiency with a maximum of 37.8 lm/W among three devices. Deep understanding of the role of HAT-CN/Al/Bphen: Li EIL in IOLEDs is necessary.

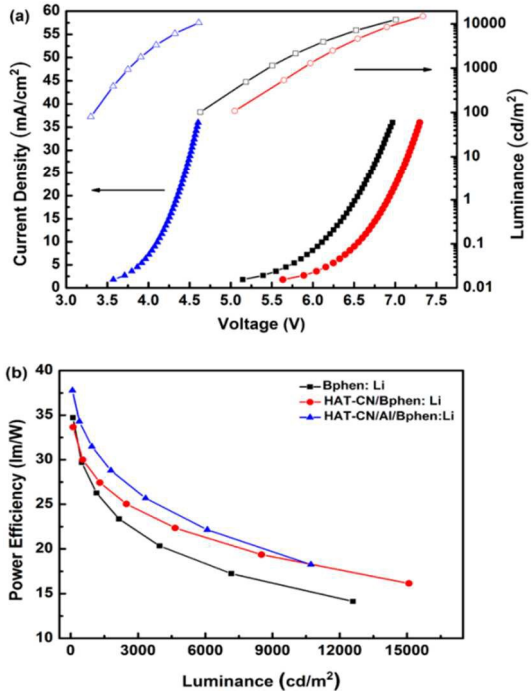


**Fig. 2** (a) Current density-voltage-luminance and (b) luminance-power efficiency characteristics of the devices with three different EILs.

Journal Name

RSCPublishing

ARTICLE

**Table 1** Electroluminescence characteristics of IOLED devices with different EILs.

| Device | Operating Voltage (V) @ 100 cd/m$^2$, 1000 cd/m$^2$, 10000 cd/m$^2$ | $\eta_p$(lm/W)[a] | CIE ($x$, $y$)[b] |
|---|---|---|---|
| Bphen: Li | 4.6, 5.4, 6.8 | 26.8 | 0.32, 0.62 |
| HAT-CN/Bphen: Li | 5.0, 5.8, 7.0 | 28.4 | 0.32, 0.62 |
| HAT-CN/Al/Bphen:Li | 3.3, 3.7, 4.5 | 31.3 | 0.31, 0.63 |

[a]Power efficiency at 1000 cd/m$^2$, [b] Commission International de I'Eclairage coordinates measured at 5 mA/cm$^2$.

Figure 3 shows the UPS spectra at the secondary electron cut-off and work function of ITO, ITO/HAT-CN and ITO/HAT-CN/Al films. The effective work function of ITO surface is calculated to be 4.78 eV. There is a small increase in the work function (by about 0.3 eV) upon the deposition of 10 nm HAT-CN on the ITO surface. It suggests that HAT-CN is a good conducting molecular layer which can effectively decrease the hole injection barrier from ITO anode. However, a 0.5 nm film of thermally evaporated Al on ITO/HAT-CN surface has a work function of 3.96 eV. To further understand the origin of the lowering voltage in HAT-CN/Al/Bphen: Li based IOLEDs, the energy levels and related electron barrier in three IOLEDs are studied by UPS.

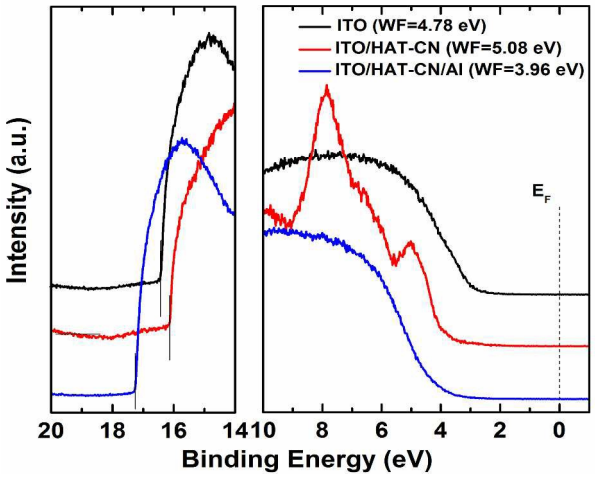


**Fig. 3** The UPS spectra for the secondary electron cutoff region and work function of the ITO, ITO/HAT-CN and ITO/HAT-CN/Al films, respectively.

Figure 4 (a) shows the HeI UPS spectra of Bphen: Li, HAT-CN/Bphen: Li, and HAT-CN/Al/Bphen: Li deposited on the ITO substrates. Corresponding energy level diagrams resulted from the UPS spectra in three devices with different EILs is summarized in Fig. 4 (b). Here, the $E_F$ of the underlying ITO substrate was measured by the UPS spectra. The HOMO level relative to the Fermi level is obtained by extrapolating in the valence band region. The vacuum level is also be calculated according to the secondary electron cut-off region. Obviously, in HAT-CN/Al/Bphen: Li based IOLEDs, there is only an electron injection barrier of 0.3 eV, which is smaller than the cases of Bphen: Li based device (1.0 eV) and HAT-CN/Bphen: Li based device (0.6 eV). The very small electron injection barrier results in the lowered driving voltage and the improved power efficiency in HAT-CN/Al/Bphen: Li based IOLEDs. Actually, 0.5 nm Al film can form islands rather than continuous films, but can obviously lower the work function of the ITO electrode. The Al thin film in the EIL is to further improve the electron injection, functions as an $n$-type doping or a trap center. This explains why the EIL with 0.5 nm Al can effectively reduce the operating voltage of IOLEDs.

To illustrate the function of EILs in IOLEDs, electron-dominated devices were fabricated to compare the effectiveness of injecting electrons from ITO cathode with different EIL to Al anode. The structures of electron dominated devices were ITO/Bphen: Li (50 nm, 1.2%)/TmPyPB (30 nm)/Al; ITO/HAT-CN (10 nm)/Bphen: Li (50 nm, 1.2%)/TmPyPB (30 nm)/Al; ITO/HAT-CN (10 nm)/Al (0.5 nm)/Bphen: Li (30 nm, 1.2%)/TmPyPB (30 nm)/Al. Hole injection is not expected from Al anode to TmPyPB due to high hole injection barrier, considering the difference between the work function of Al (≈ 4.3 eV) and the HOMO of TmPyPB (≈6.7 eV). Figure 5 shows a plot of the current density versus voltage of electron dominated devices. The devices with HAT-CN/Al/Bphen: Li EIL shows higher current density than other devices at the same driving voltage. It suggests that the electron capability of HAT-CN/Al/Bphen: Li EIL is stronger than HAT-CN/Bphen: Li and Bphen: Li EIL. Furthermore, the electron injection efficiency in three different EIL based devices were calculated as shown in

the inset of Fig. 5. The injection efficiency, $J_{INJ}$, was determined by the equation:[22-24]

$$\eta_{INJ} = J_{INJ}/J_{SCL} \quad (1)$$

where the $J_{INJ}$ is the measured current density, and $J_{SCL}$ is the

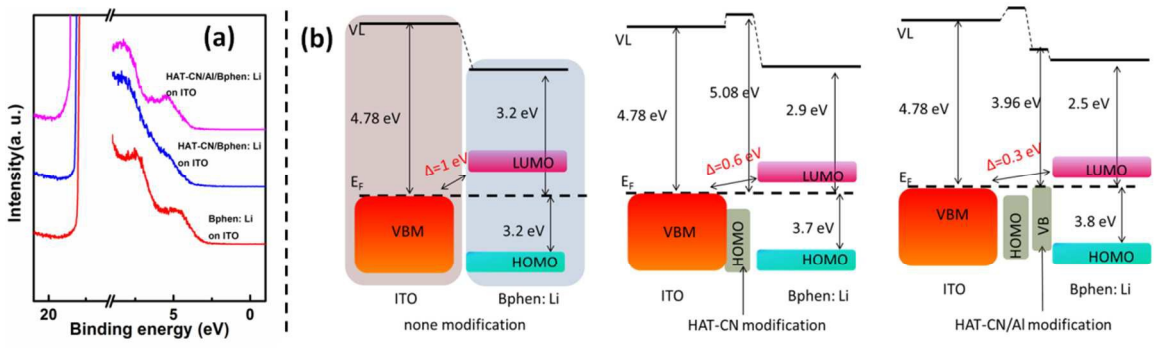


Fig. 4 (a) Hel UPS spectra of Bphen: Li, HAT-CN/Bphen: Li, and HAT-CN/Al/Bphen: Li interfaces on the ITO substrates. (b) Schematic energy level diagrams of ITO/Bphen: Li, ITO/HAT-CN/Bphen: Li, and ITO/HAT-CN/Al/Bphen: Li interfaces on an ITO substrate.

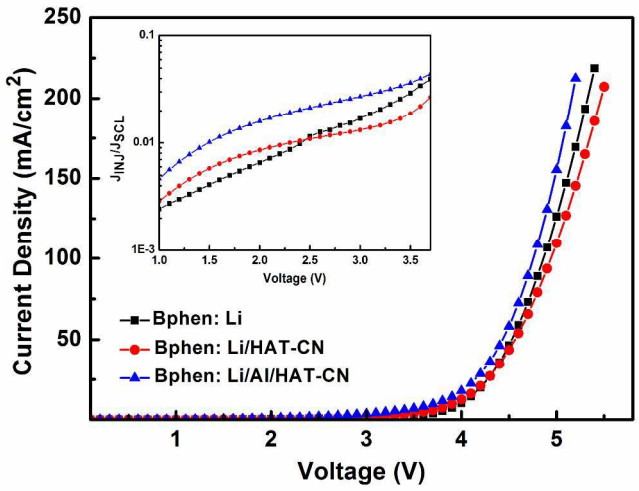


**Fig. 5** Current density-voltage characteristics of the devices with three different EILs. Inset is the electron injection efficiency plots in three different EIL deivces.

calculated theoretical space-charge-limited current (SCLC) density. As expected, HAT-CN/Al/Bphen: Li EIL exhibits higher injection efficiency than that of other EILs.

We also prepared 120×120 mm$^2$ flexible IOLED panels on PET/ITO substrates by utilizing HAT-CN/Al/Bphen: Li EIL. Figure 6 (a) shows the top-view photograph of flexible green phosphorescent IOLED panel. The flexible PET substrates have a thickness of about 60 μm (side-view shown in Fig.6 (b)). Uniform and bright luminance in a large flexible panel is realized by using this efficient EIL interfacial layer. Since the advantage of lower driving voltage, HAT-CN/Al/Bphen: Li EIL based IOLEDs demonstrate a potential application in commercial flexible lighting panel in the future. Unfortunately, the luminance characteristics of the fabricated large-area panels was not measured successfully presently due to the large issue of encapsulation techniques for large-area flexible panels. Great efforts to develop efficient encapsulation techniques for flexible panels are necessary in the future.

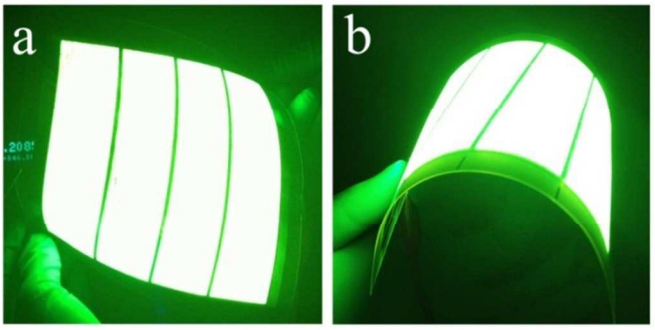


**Fig. 6** (a) Top and (b) side view images of green phosphorescent IOLED fabricated on large-area flexible substrate (120×120 mm$^2$).

## Conclusions

In summary, a HAT-CN/Al/Bphen: Li interlayer between ITO cathode and ETL for inverted OLEDs is developed and the effect on electron injection has been demonstrated. The IOLEDs with HAT-CN/Al/Bphen: Li interlayer demonstrated very low driving voltage of 4.5 V at 10000 cd/m$^2$, which is the lowest value of green phosphorescent IOLEDs to date. Based on the interlayer, we fabricated a large-area flexible green phosphorescent IOLED with active area of 120×120 mm$^2$, which shows the outstanding potential to construct the solid state lighting fabrication.

## Acknowledgements

We acknowledge financial support from the Natural Science Foundation of China (Nos. 61307036 and 61177016) and from the Natural Science Foundation of Jiangsu Province (No. BK20130288). This project is also funded by the Collaborative Innovation Center of Suzhou Nano Science and Technology,

and by the Priority Academic Program Development of Jiangsu Higher Education Institutions (PAPD).

## Notes

Jiangsu Key Laboratory for Carbon-Based Functional Materials & Devices, Institute of Functional Nano & Soft Materials (FUNSOM), and Collaborative Innovation Center of Suzhou Nano Science and Technology, Soochow University, Suzhou, Jiangsu 215123, China

Email: lsliao@suda.edu.cn; zkwang@suda.edu.cn

‡These two authors contributed equally to the work.

## References

1 S. Reineke, F. Lindner, G. Schwartz, N. Seidler, K. Walzer. B. Lüssem and K. Leo, *Nature*, 2009, **459**, 239.
2 L.-S. Liao, W.-K. Slusarek, T.-K. Hatwar, M.-L. Ricks and D.-L. Comfort, *Adv. Mater.*, 2008, **20**, 324.
3 E.Fortunato, P. Barquinha and R. Martins, *Adv. Mater*, 2012, **24**, 2945.
4 K.-A. Knauer, E. Najafabadi, W. Haske and B. Kippelen, *Appl. Phys. Lett.*, 2012, **101**, 103304.
5 L. Xiao, Z. Chen, B. Qu, J. Luo, S. Kong and J. Kido, *Adv. Mater.*, 2011, **23**, 926.
6 H. Ishii, K. Sugiyama, E. Ito and K. Seki, *Adv. Mater.*, 1999, **11**, 972.
7 A. Kahn, W. Zhao, W. Gao, H. Vazquez and F. Flores, *Chem. Phys.*, 2006, **325**, 129.
8 C.-I. Wu, C.-T. Lin, Y.-H. Chen, M.-H. Chen, Y.-J. Lu and C.-C. Wu, *Appl. Phys. Lett.*, 2006, **88**, 152104.
9 Z. K.Wang, Y.H. Lou, S. Naka, Okada. H, *ACS Appl. Mater. Interfaces*, 2011, 3, 2496.
10 S. Tsang, Z. Lu and Y. Tao, *Appl. Phys. Lett.*, 2007, **90**, 13211.
11 S. Braun, W.-R. Salaneck and M. Fahlman, *Adv. Mater.*, 2009, **21**, 1450.
12 W. Chen, D. Qi, X. Gao and A. T. S. Wee, *Prog. Surf. Sci.*, 2009, **84**, 279.
13 F. Wang, T. Xiong, X.Qiao and D. Ma, *Org. Electron.*, 2009, **10**, 266.
14 Z. K. Wang, Y. H. Lou, S. Naka, H. Okada, *Appl. Phys. Lett.*, 2011, 98, 063302.
15 J. Kido and T. Matsumoto, *Appl. Phys. Lett.*, 1998, **73**, 2866.
16 N. Koch, S. Duhm, J.-P. Rabe, A. Vollmer and R.-L. Johnson, *Phys. Rev. Lett.*, 2005, **95**, 237601.
17 H. Kanno, R.-J. Holmes, Y. Sun, S. K. Cohen and S.-R. Forrest, *Adv. Mater.*, 2006, **18**, 339.
18 M.-Y. Chan, S.-L. Lai, K.-M. Lau, M.-K. Fung, C.-S. Lee and S.-T. Lee, *Adv. Funct. Mater.*, 2007, **17**, 2509.
19 D.-S. Leem, H.-D. Park, J.-W. Kang, J.-H. Lee, J.-W. Kim and J.-J. Kim, *Appl. Phys. Lett.*, 2007, **91**, 011113.
20 C. H. Gao, S. D. Cai, W. Gu, D. Y. Zhou, Z. K. Wang, L. S. Liao, *ACS Appl. Mater. Interfaces*, 2012, 4, 5211.
21 J.-H. Lee, J.-W. Kim, S.-Y. Kim, S.-J. Yoo, J.-H. Lee and J.-J. Kim, *Org. Electron.*, 2012, **13**, 545.
22 P. -N. Murgatroyd, *J. Phys. D: Appl. Phys.*, 1970, **3**, 151.
23 C.-E. Small, S.-W. Tsang, J. Kido, S.-K. So and F. So, *Adv. Funct. Mater.*, 2012, **22**, 3261.
24 C.-H. Gao, X.-Z. Zhu, L. Zhang, D.-Y. Zhou, Z.-K. Wang and L.-S. Liao, *Appl. Phys. Lett.*, 2013, **102**, 153303.